Effect of Gap Ratio on the Wake behind Two Side-by-Side Flat Plates

B. Shin[1†] and M. Kondo[2]

[1] *Department of Mechanical Design Systems Engineering, University of Miyazaki, Miyazaki, 889-2192, Japan*
[2] *Graduate School of Engineering, University of Miyazaki, Miyazaki, 889-2192, Japan*

†*Corresponding Author Email: brshin@cc.miyazaki-u.ac.jp*

ABSTRACT

The flow behind two flat plates placed normal to the flow in side-by-side arrangement was experimentally investigated by varying the gap ratio G^* (the ratio of gap spacing to plate width) in the range of $0.0 \leq G^* \leq 2.5$ to examine the effect of gap ratio on the wake. The flow patterns around the plates were observed using the hydrogen bubble flow visualization in the water tunnel. Velocity and pressure components were acquired by employing hot-wire anemometers and digital manometers in the wind tunnel. From the experiment, it has been found that, at gap ratios less than 1.6, the gap flow was biased either upward or downward and maintained a stable biased flow pattern. The width of the wake on the biased side was increased with the gap ratio, while that on the unbiased side was decreased. At $1.6 \leq G^* < 2.0$, the switching of the biased gap flow appeared due to the flow instability by mutual interference of the vortex shedding from the plates, while at G^* of 2.0 or more, the gap flow was no longer biased. The plates on the biased side showed relatively low base pressure and high velocity, and detected periodic vortex shedding, while those on the unbiased side showed the opposite phenomena. At gap ratios less than 2.0, two Strouhal numbers indicating the bi-stable situation exist, and the difference between the two Strouhal numbers decreased with the gap ratio.

Keywords: Wake; Vortex interference; Two flat plates; Side-by-Side arrangement.

NOMENCLATURE

Cp	pressure coefficient		u	streamwise velocity
D	plate width		u'	u-velocity fluctuation
f	frequency of the u-velocity fluctuation		x	streamwise coordinate
G	gap spacing between the plates		y	cross-stream direction coordinate
G^*	gap ratio			
p	static pressure on the flat plate		ρ	density of fluid
p_∞	static pressure of free stream		ν	kinematic viscosity of fluid
Re	Reynolds number			
R_τ	cross correlation coefficient		Subscripts	
St	Strouhal number		*in*	inner edge
U	uniform inlet velocity		*out*	outer edge

1. INTRODUCTION

The flow around a bluff body has been a topic of considerable interest in the fields of engineering and fluid dynamics. From an engineering viewpoint, this type of flow is commonly encountered and widely discussed in many branches of engineering such as mechanical, civil, and oceanographic engineering for design of heat exchangers, bridges, and marine structures. From a fluid dynamics point of view, it presents various physical phenomena such as flow separation, vortex shedding, shear layer instability, flow induced vibration. When a bluff body comprised of multiple objects is placed in a flow, it has been revealed that the wake and vortices interfere with each other based on the arrangement of objects, so that the fluid forces and vortex shedding frequencies acting on the object show a large difference compared to that of a single object (Spivack *et al.*, 1946; Bearman and Wadcock, 1973; Williamson, 1985; Zdravkovich, 1987). Research on this mutual interference has been mainly conducted

by the experimental approach on the flow behind one or multiple circular cylinders and has elucidated various relevant flow phenomena (Sumner, 2010; Zhao and Cheng, 2014; Carini *et al*., 2014; Tong *et al*., 2015; Zhou and Alam, 2016; Alam *et al*., 2017). It is known, for example, that, when two side-by-side cylinders are placed normal to the flow and the gap spacing between the cylinders is larger than the diameter of the cylinder, the vortex shedding frequency from each cylinder is similar to that of single cylinder, but if smaller, the two cylinders show different vortex shedding frequencies and fluid forces, and the interference of wakes occurs, so that the bi-stable asymmetric wake characteristic can be realized (Kim and Durbin, 1988; Alam *et al*., 2003; Wang and Zhou, 2005). In order to investigate the nature of the interference, Kamemoto (1976) theoretically analyzed the instability of the wakes by using the flow model with two parallel vortex sheets. As a result of these studies, our understanding of the wake flow behind the cylinder has been greatly improved.

On the other hand, studies on bluff bodies with multiple square cylinders (Liu and Chen, 2002; Yen and Liu, 2011; Alam *et al*., 2011; Burattini and Agrawal, 2013; Han *et al*., 2014; Chatterjee and Biswas, 2015) or flat plates has received little attention even though most structures around us are slender structures with quadrilateral cross sections. Especially, a limited number of studies on the flow around multiple flat plates have been reported (Hirano *et al*., 1983; Williamson, 1985; Hayashi *et al*., 1986; Miau *et al*., 1992; Higuchi *et al*., 1994; Hacisevki and Teimourian, 2015; Teimourian *et al*., 2017). For the flow normal to the flat plates in side-by-side arrangement, for example, Hayashi *et al*. (1986) conducted experimental investigation of the wake interference of a row of multiple flat plates by the visualization and showed that the gap flow could be classified into three flow patterns depending on the gap ratio: biased flow in the same direction, flip-flopping flow and unbiased flow. Also, through estimation of aerodynamic characteristics such as drag, base pressure and Strouhal number in wind-tunnel experiments, Hayashi *et al*. (1986) have explained the relationship of these characteristics to the three patterns, and concluded that the plates on the biased side showed high drag and regular vortex shedding, while those on the unbiased side showed the opposite. They assumed that the origin of biasing is related to the vortex shedding of each plate. However, there is no experimental evidence such as temporal information on velocity and pressure. Miau *et al*. (1992) experimentally studied the downstream flow between two flat plates in parallel arrangement with gap ratios between 1.5 and 1.85, and discussed the gap flow switching in detail by introducing velocity fluctuations. They have shown that periodic vortex shedding was detected at the outer edges of the wake shear layer on the biased side of the gap flow but no periodic vortex shedding was measured on the unbiased side. From previous works (Hirano *et al*., 1983; Williamson, 1985; Hayashi *et al*., 1986; Miau *et al*., 1992), we know well that there is appearance of a transition between bi-stable asymmetric wake and symmetric wake at gap ratios

less than 2.0. However, most of the fluid dynamic aspects such as interference phenomena of wakes and switching of the gap flow still remain to be clarified. In particular, the asymmetrical flow regime has not been investigated fully. It is the motivation of this research.

The objective of this paper is to explore the effect of gap ratio on the wake flow behind two flat plates placed normal to the flow in side-by-side arrangement. To attain this end, experimental investigation was conducted by varying the gap ratio mainly in the asymmetrical flow regime at a Reynolds number of 8000. First, in order to investigate the relationship between the gap ratio and wake pattern, the behavior of the gap flow and the spatial development of the wake, careful observation of wake flow by visualization was performed in the water tunnel and depicted with a realized image. Then, in order to identify the wake flow characteristics between the flows with and without the gap flow switching, velocity and base pressure were measured in detail by employing hot-wire anemometers and digital manometers in the wind tunnel and analyzed.

2. EXPERIMENTAL DETAILS

2.1 Flow Visualization in a Water Tunnel

Flow visualization was performed in a circulating water tunnel with a test section of 4.0m x 0.4m x 0.6m, and the water depth of 0.4m as shown in Fig. 1 by using hydrogen bubble flow visualization technique. The flow is driven using an impeller, and the flow velocity, U, is controlled by a computer at a range of 0.09~1.0m/s. For rectification, 1.0m x 0.4m perforated plate and stainless mesh was installed. In order to suppress surface waves, a wave-suppressor-plate was placed at the entrance of the test section. The turbulence intensity at the core region excluding the water surface and near the walls was lower than 1.0%. Two aluminum flat plates arranged side-by-side were mounted normal to the flow and perpendicular to the water surface, and the gap spacing between the plates was able to be controlled freely according to the gap ratio, G^* (the ratio of gap spacing (G) to plate width (D)). Each of the flat plate with rectangular cross section was 30mm wide and 3mm thick, and its effective span was 550mm. To generate the hydrogen bubbles, a 100μm diameter copper wire cathode was placed in front of the plates, and the voltage between the cathode and anode was controlled by a DC stabilized power supply (Takasago LX035-1B). The visualized flow field by the hydrogen bubbles was illuminated with a light sheet parallel to the flow direction using a display projector (MASTER BenQ, MW712), and recorded using a video camera (Panasonic HDC-TM70). The recording time was 3 minutes per experiment.

2.2 Wind Tunnel Experiments

Hot-wire experiments were carried out in the multi-fan type wind tunnel of University of Miyazaki. The tunnel is composed of a series of 99 fans arranged in a grid-like pattern (9 columns x 11 rows), and each

fan is individually controlled through separate AC servo-motors. The test section measures 15.5m long (adjustable), 2.6m wide and 1.8m high, and the maximum wind velocity is up to 16m/s. Several experiments utilizing this facility have shown its efficacy in generating and reproducing various statistical characteristics of gas flows in some published papers (e.g. Ozono *et al*., 2006; Butler *et al*., 2010; Pan *et al*., 2011). To obtain good homogeneity in uniform flow, the input signals were tuned carefully. After the calibration, the non-homogeneity of the mean streamwise velocity is less than ±2%, and the turbulence intensity is less than 2.0 %.
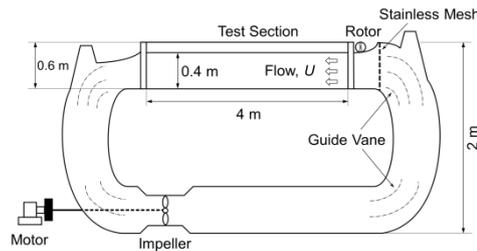
Fig. 1. Side view of the water tunnel.

Figure 2 schematically depicts the experimental setup. It was placed 10m downstream from the entrance of the test section. The center of two flat plates, identical to ones used in the water tunnel experiments, was placed 625mm above the floor of the wind tunnel, and the gap spacing was varied freely according to the gap ratio. Also, in order to preserve two-dimensionality of the flow, two tapered end plates 12mm thick, 1m long and 1.8m high were placed parallel to the flow direction. A two-dimensional traverser was installed in order to shift the sensor to its required position.
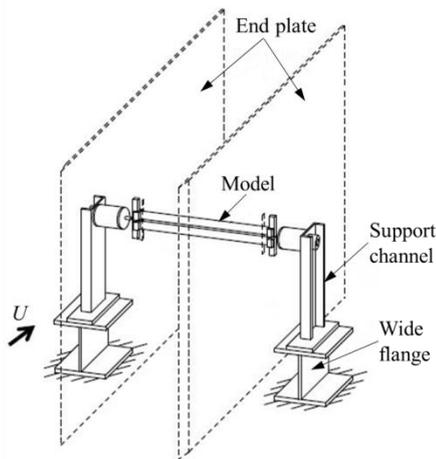
Fig. 2. Experimental setup.

The velocity fluctuations behind the flat plates with gap ratio in the range of $1.5 \leq G^* \leq 2.5$ was mainly measured using a constant-temperature hot-wire anemometer (Kanomax CTA 1011). In order to investigate the velocity distribution without the

switching phenomena of gap flow, the flow at $G^*=0.8$ was also measured. An I-wire probe (Model 1210) was mounted on a computer-controlled traverse. The probes had a nominal length of 1.0 mm. The hot-wire signals were digitized via an AD convertor (KEYENCE NR-600), and analyzed on a personal computer. Power spectral density analysis was performed by means of Fast Fourier Transform (FFT). The sampling frequency was set at 500Hz and signals were captured for duration of 2 or 20 minutes for each experiment. The uniform inflow velocity, U, was set to 4.0m/s and the corresponding Reynolds number (Re) based on U and D was 8000 (Hayashi *et al*., 1986; Miau *et al*., 1992), because it is well known that at Reynolds number over 5000, the characteristics of the flow behind the plates do not depend too much on the Reynolds number (Flachsbart, 1935; Nakaguchi, 1972; Hirano *et al*., 1983; Okajima and Sugitani, 1984; Hayashi *et al*., 1986).

Figure 3 depicts the arrangement of flat plates, coordinate system, flow parameters and measuring points of velocity and pressure behind the two plates. Two hot-wire probes were situated at $x = 2D$, one of which was situated at $1/3D$ upward from the upper edge of the plate, slightly outside of a wake shear layer (hereafter called "outer edge") and the other was situated at downward from the other edge in the gap side (called "inner edge"). This location was determined by observing the velocity fluctuations with traversing the probe, such that the probe could clearly sense the velocity fluctuations in the shear layer of the wake flow, regardless of whether the gap flow deflects toward either side (Bradbury, 1976; Mizota, 1978).
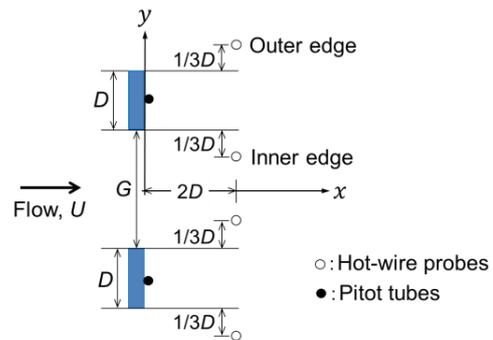
Fig. 3. Arrangement of two normal flat plates and measuring points.

3. RESULTS AND DISCUSSION

3.1 Flow Visualization around Two Side-by-Side Flat Plates

The visualization experiment was conducted at a gap ratio of $0.0 \leq G^* \leq 2.5$ at intervals of 0.1. Figure 4 shows instantaneous wake flow patterns visualized by hydrogen bubble flow visualization for gap ratios of G^* = 0.1, 0.4, 0.8, 1.2, 1.6, 1.8, 2.0, 2.5. The Reynolds number defined by uniform inlet velocity and the width of the flat plates was 8000 (U = 0.27m/s).
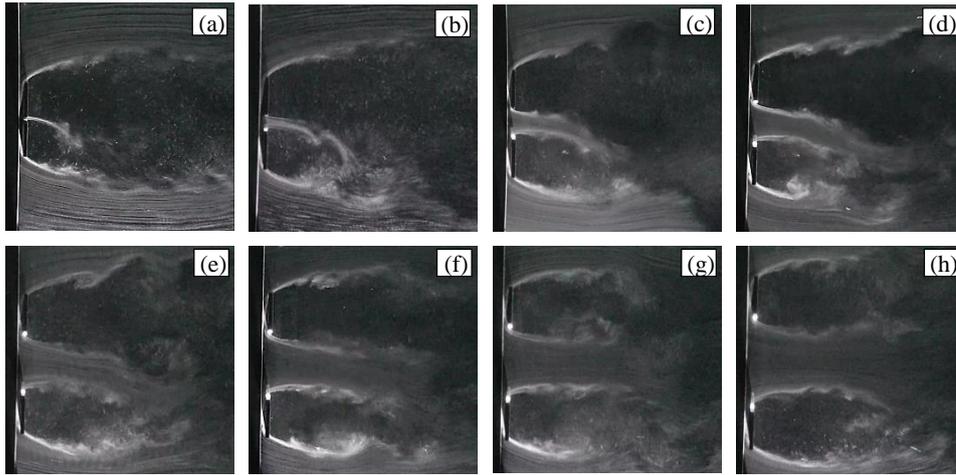
Fig. 4. Flow behind two flat plates at *Re* = 8000, (a) $G^* = 0.1$, (b) $G^* = 0.4$, (c) $G^* = 0.8$, (d) $G^* = 1.2$, (e) $G^* = 1.6$, (f) $G^* = 1.8$, (g) $G^* = 2.0$ and (h) $G^* = 2.5$.

At gap ratios of $0.1 \leq G^* < 1.6$, the gap flow was deflected either upward or downward (Hayashi *et al.*, 1986) and unless disturbed by an external force, showed a stable flow pattern while staying bias. The bias direction could be changed by applying disturbance, but after the change in direction it became a new stable biased flow pattern. This is a different flow phenomenon seen from the gap flow between two cylinders arranged side-by-side (Zhou and Alam, 2016; Carini *et al.*, 2014), which irregularly changed directions due to instability. Furthermore, this bias phenomenon was clearly different from the Coanda effect deflecting along a curved surface such as a cylinder. The degree of bias decreased as G^* increased, and due to the bias, naturally a narrow wake region on the biased side of the gap flow and a wide wake region on the unbiased side were formed behind the two flat plates. Also, the size of the narrow wake was increased with the gap ratio, while that of the wide wake was decreased. In small gap ratios, for example $G^* = 0.1$ (Fig. 4(a)), the vortex shedding from the separated shear layers by the outer edge of both plates was distinct, but vortex formation is not clear in the gap flow. At ranges of around $G^* = 0.2{\sim}1.6$, the vortex formation and shedding from the flat plate on the narrow wake side became active with rolling up the shear layer that was separated from two edges of the plate. Also, it was observed that the vortex which formed from the shear layer by the inner edges of two plates (on the gap side) was engulfed by the vortex that formed from the outer edge of the plate on the narrow wake side (Figs. 4(b)-(d)). On the other hand, it was observed that typical Kelvin-Helmholtz-like vortices were formed in the separated shear layer from the outer edge of the plate on the wide wake side and flowed toward downstream interfering with the vortices formed on the narrow wake side. But, the roll up of shear layer into the wake behind this plate could not be observed.

At gap ratios of $1.6 \leq G^* < 2.0$, the gap flow became unstable and a flip-flopping phenomenon in which the bias of gap flow irregularly switches up and down appeared randomly(Hayashi *et al.*, 1986; Miau *et al.*,

1992). Further, it was observed that, although the separated shear layer from the gap side of the plate on the wide wake side is strongly affected by the vortex shedding on the narrow wake side (Figs. 4(e) and (f)), this shear layer could roll up into its own wake and shed distinct vortices. It seems that the vortex shedding from individual plates stimulates the gap flow and destabilizes the gap flow biasing, and is considered to be the cause of the flip-flopping phenomena. The switching peaked around $G^* = 1.7$ when seen by eye. Also, it was found that the difference in periods of vortex shedding and the width of the wake between the biased and unbiased sides gradually decreased as the gap ratio increased.

At ranges of $G^* \geq 2.0$, biased gap flow did not appear. Individual wakes almost identical to each other were formed behind the two flat plates, and showed almost symmetric wake flow pattern (Figs. 4(g) and (h)).

As investigated so far, it has been confirmed that the gap ratio had a strong influence on the wake behind two flat plates, and three flow regimes with different gap flow patterns have been found according to the gap ratio. As the gap ratio increased, the wake region behind the flat plate on the narrow wake side increased in size until the width of the wakes behind two plates reached the same level, so that the difference between the sizes of the wakes became reduced.

3.2 Spectral Signals and Strouhal Numbers

Wind tunnel experiments were conducted to investigate the velocity fluctuation as well as base pressure of the wake behind the two flat plates. For this end, the experiment was done 20 times for a duration of 2 minutes each, and data were obtained from the inner and outer edges at $x = 2D$ downstream of the flat plates as illustrated in Fig. 3. The predominant frequencies of vortices generated by the two flat plates and their interference may be extracted from the power spectral density (PSD) of velocity. Figure 5 shows the PSD of hot-wire signals by FFT analysis mainly in the regime of gap flow switching. Here, PSD was determined by the average
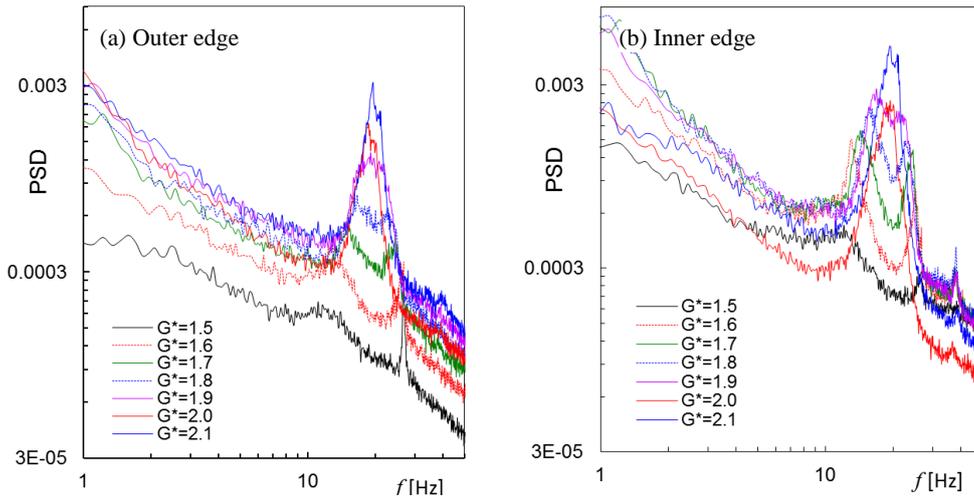
Fig. 5. Power spectral density of the streamwise velocity fluctuation at (a) the outer edge, (b) the inner edge and *Re* = 8000.

of 20 FFT results, where each result composed of 4096 (10^{12}) samples. It can be seen that at $G^* < 2.0$, two distinct peaks appeared and the difference of frequencies between the first and second peaks decreased with the gap ratio. As investigated in Fig. 4, it implies that the difference in periods of vortex shedding and in size of width of the wakes between the biased and unbiased sides gradually decreased with the gap ratio. However, when $G^* \geqq 2.0$, even though a weak second peak is shown, almost a single pronounced peak occurred; that is, vortices are shed at the same frequency from the two plates. Also, at around $G^* = 1.9~2.0$, the PSD showed a transition from the flow with the two distinct peaks and that with the single peak. Overall, the PSD of the two peaks at the inner edge (Fig. 5(b)) is stronger and more pronounced than that at the outer edge (Fig. 5(a)). Figure 6 shows the distribution of Strouhal numbers ($St = fD/U$) estimated by the frequencies corresponding to the pronounced peaks in Fig. 5 in the ranges of $1.5 \leq G^* \leq 2.5$. As can be seen from this figure, at regions $G^* < 2.0$ where asymmetric wake occurs due to the biased flow, two different Strouhal numbers appeared as noted in Fig. 5. This is due to the existence of both high and low frequencies of vortex shedding by the mutual interference between the narrow and wide wake. As seen from the results in Fig. 4, the higher St is due to the relatively small scale and strong vortex shedding from the flat plate on the narrow wake side, and the lower St is due to the vortex shed slowly from the wide wake side. It showed that the higher St tends to decrease as the gap ratio increases because frequencies of vortex shedding are decreased by increasing the size of the wake with the gap ratios, while the lower St increases. This relationship agrees well with Roshko's (1955) results which reported that the vortex shedding frequencies around bluff bodies is inversely proportional to the widths of wakes. The presence of these two different Strouhal numbers indicates that the asymmetric wake is in a bi-stable situation (Spivack, 1946; Hayashi *et al.*, 1986; Kim and Durbin, 1988; Chen *et al.*, 2003). In this bi-stable regime, the difference between the higher and lower

Strouhal numbers decreases as the gap ratio increased. At ranges $G^* \geqq 2.0$, where the gap flow is no longer biased (Hayashi *et al.*, 1986), as a whole, each plate shed a pair of vortices at approximately similar frequencies. The Strouhal numbers show vortex shedding behavior almost like that of a single flat plate even though, at $2.0 \leq G^* \leq 2.3$, there were observed very weak higher St represented by broken symbols corresponding to the pronounced second peaks of frequencies. Therefore, it is assumed that mutual interference between wakes from plates on both biased and unbiased sides is weak.
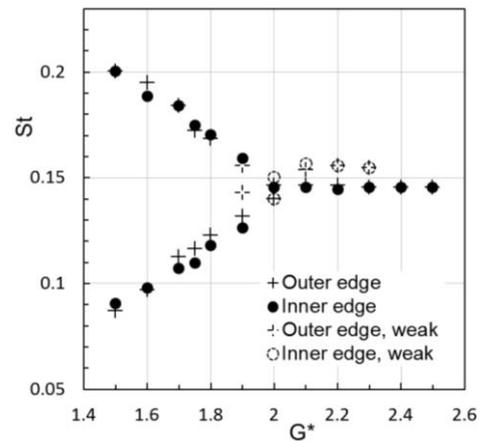
Fig. 6. Strouhal numbers with G^* at $x = 2D$.

3.3 Velocity and Base Pressure Distribution at Flow without Gap Flow Switching

Figure 7 shows time histories of velocity and base pressure coefficient signals at $G^* = 0.8$ as an example of the flow without the gap flow switching. Since the biasing of gap flow is stable in either side in this gap ratio, experiments were conducted by alternating for the two flat plates. Two hot-wire probes were fixed in two locations of the outer edge and inner edge of

(a) Wide wake side   (b) Narrow wake side
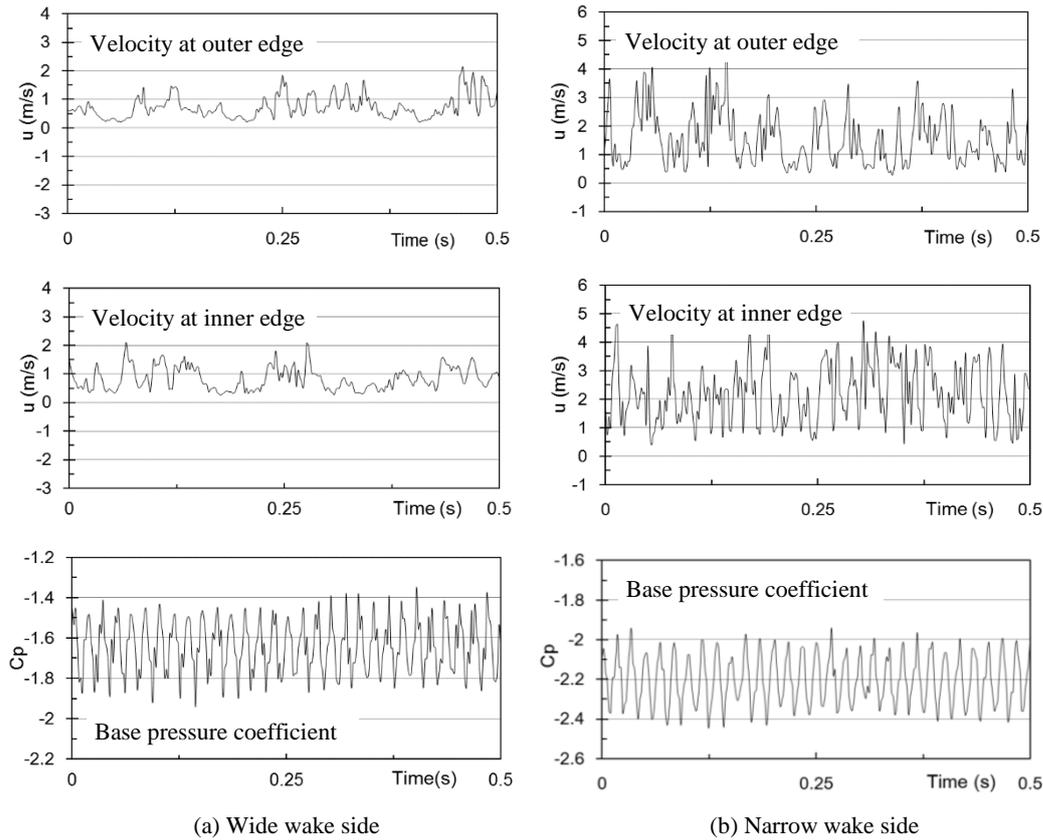
Fig. 7. Time histories of velocity and base pressure coefficient signals behind the flat plate at $G^* = 0.8$.

each flat plate at $x = 2D$ downstream as shown in Fig. 3. The base pressure was measured by attaching a pressure tab at the center of the back surface of each plate. These figures show a 0.5-second signal among the data measured several times for duration of 20 minutes each.

Figure 7(a) shows raw signals of u-velocity and pressure coefficient behind the flat plate on the wide wake side and Fig. 7(b) shows those on the narrow wake side. Here, the pressure coefficient was calculated using the static pressure obtained on the back surface of each plate and dynamic pressure from the uniform inflow velocity U, Cp=2(p-p∞)/ρU2. Even if measuring points were placed at the same downstream from the plates, the velocity on the wide wake side (Fig. 7(a)) was relatively weak and the wave pattern was also irregular. However, a periodic-like flow appeared on the narrow wake side (Fig. 7(b)). Therefore, from these figures and Fig. 4, it can be deduced that a large scale wake in width and length formed on the unbiased side. As a whole, the velocity at the gap side (inner edges) is higher, and at the outer edges of both flat plates, the velocity on the narrow wake side is higher than that on the other side. On the other hand, pressure showed to be lower at the narrow wake side, and its signal on this side also tends to be distributed regularly than those on wide wake side, matching the frequency of the vortex shedding. As can be seen in Fig. 4, this corresponds to that the flat plate on the narrow wake side makes more active vortex formation and shedding.

3.4 Velocity and Base Pressure Distribution at Flow with Gap Flow Switching

Figure 8 shows time histories of velocity fluctuation and base pressure coefficient signals at G^*=1.75, in which the active occurrence of gap flow switching showed around this gap ratio in the previous flow visualizations. The data was obtained at the same locations as Fig. 7, but since this flow accompanies gap flow switching, the flow behind only one flat plate was measured. As in the previous section, these figures show a 0.5-second signal when the characteristic pattern of signal was seen by the bias of gap flow. Figure 8(a) shows raw signals of velocity fluctuation and pressure coefficient when the width of wake behind the flat plates became wide by the gap flow switching and Fig. 8(b) shows the signals when the width became narrow. Very complicated velocity fluctuations with turbulent behavior appeared on the wide wake side in Fig. 8(a), whereas periodicity in the velocity fluctuation traces with the frequency and amplitude being nearly constant was seen on the narrow wake side in Fig. 8(b). This could be seen from the cross correlation coefficient (R_τ) shown in Fig. 9. Here, R_τ is defined by $R_\tau = \overline{u'_{out}(t)u'_{in}(t+\tau)} / \{(\overline{u'^2_{out}})^{1/2}(\overline{u'^2_{in}})^{1/2}\}$ (Kundu *et al.*, 2012), where u'_{out} and u'_{in} correspond to the random velocity fluctuation at the outer edge and inner edge, respectively and time t. τ is the time lag, and the over bar refers to the ensemble average in this case. Figure 9(a) indicates the correlation
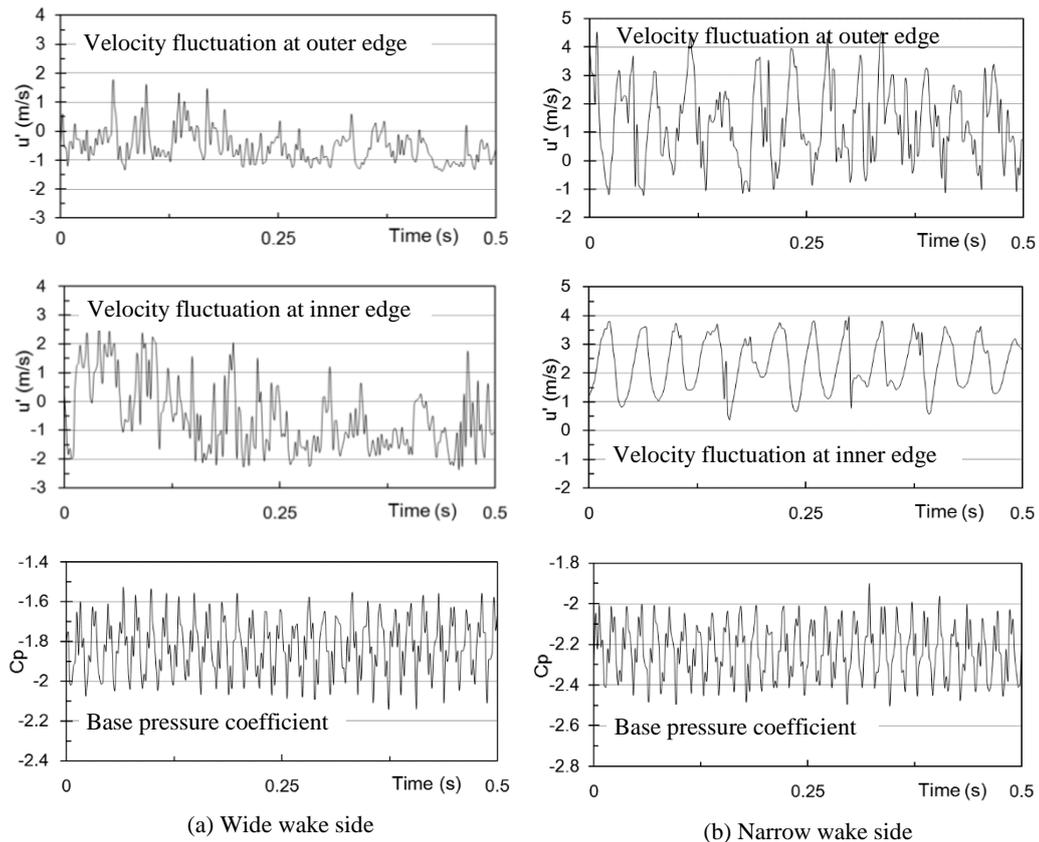
Fig. 8. Time histories of velocity fluctuation and base pressure coefficient signals behind the flat plate at $G^* = 1.75$.

coefficient obtained from the velocity fluctuation on the wide wake side corresponding to the Fig. 8(a), and Fig. 9(b) indicates that on the narrow wake side corresponding to the Fig. 8(b). It could be seen that the R_τ in Fig. 9(b) shows much more periodic fluctuation than that in Fig. 9(a) presenting turbulent velocity fluctuations. From Fig. 8, it can be seen that when the gap flow biased, the velocity on the narrow wake side becomes higher than the time averaged velocity, and the amplitude of the velocity fluctuation at the gap side is smaller than that of the outer side near the wake shear layer. However, in the case of the wide wake side, these correlations reverse. The velocity fluctuation was most intense near the wake shear layer on the outer edge on the narrow wake side. On the other hand, it could be understood that the base pressure distribution on the narrow wake side flat plate is lower than that on the wide wake side, suggesting that the drag on the narrow wake side becomes high. As an example of the gap flow switching, Fig. 10 shows the change in velocity fluctuation as well as pressure coefficient with time when the width of the wake switches from a wider state to a narrow state (Fig. 10(a)), and vice versa (Fig. 10(b)), which signifies that the gap flow is switching from one side to the other. It could be clearly seen that the flow characteristics investigated in Fig. 8 appears as it is: the velocity fluctuation and pressure coefficient gradually changes with the gap flow direction. Miau *et al.* (1992) also reported this switching flow characteristic for the flow at $Re = 6600$. However, there is no information related to

pressure and the magnitude of velocity is uncertain in their works.
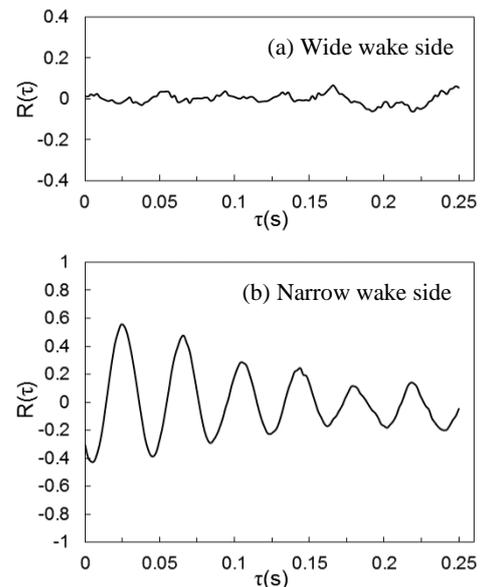
Fig. 9. Cross correlation coefficients for velocity fluctuations corresponding to the Fig.8.

4.   CONCLUSION

The wake flow behind two flat plates arranged side-
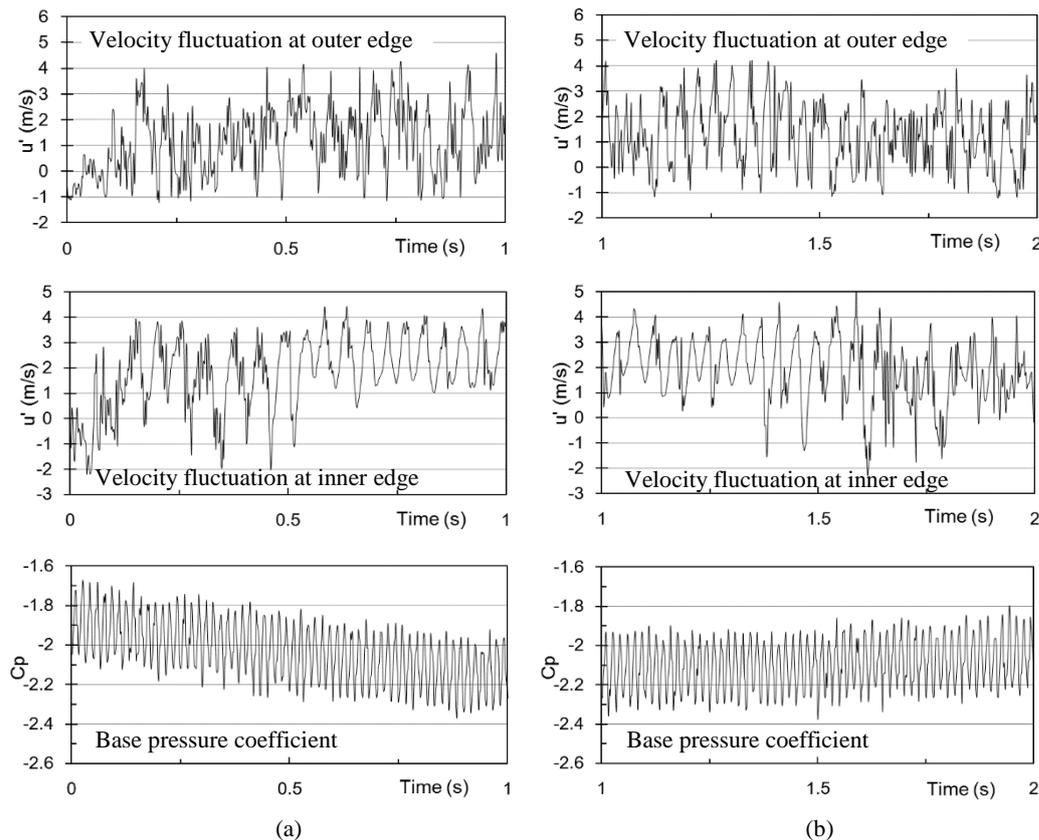
Fig. 10. Time histories of velocity fluctuation and base pressure coefficient signals behind the flat plate during gap flow switching at $G^* = 1.75$.

by-side was experimentally investigated by varying the gap ratio G^* in the range of $0.0 \leq G^* \leq 2.5$ at Reynolds numbers of 8000 to explore the effect of gap ratio on the wake. The flow patterns around the plates were observed using the hydrogen bubble flow visualization in the water tunnel. Velocity and base pressure were obtained by using hot-wire anemometers and digital manometers in the wind tunnel. From the experiments, it has been confirmed that the gap ratio had a strong influence on the wake behind two flat plates. The main results of this study can be summarized as follows.

At gap ratios of $0.1 \leq G^* < 1.6$, the gap flow was stably biased towards either the upper or the lower plate. At $1.6 \leq G^* < 2.0$, the gap flow switching appeared due to the flow instability by mutual interference of the vortex shedding from each plate. Also, both high and low Strouhal numbers appeared in this regime of G^*. The difference between the higher and lower Strouhal numbers decreased as the gap ratio increased. At ranges $G^* \geqq 2.0$, where the gap flow showed no bias, each plate shed a pair of vortices at similar frequencies. It was found that the scale of the wake on the biased side of the gap flow increased with the gap ratio, while that on the unbiased side decreased until the width of the wakes behind two plates reached the same level. The plates on the biased side showed relatively low base pressure and detected periodic vortex shedding, while those on the unbiased side showed the opposite

phenomena. It was also shown that time averaged velocity on the biased side was higher than that on the unbiased side, and the velocity on the inner edges of each flat plate was also higher than that on the outer edges.

For a better understanding of the asymmetric vortex flow phenomena and its effects, further investigation related to the fluid dynamics force and moment exerted on the plates, and coherent vortex shedding structure in the wake region will be needed. Moreover, investigation of the vortex formation process and the spatial distribution of velocity and pressure using computational fluid dynamics will be necessary.

REFERENCES

Alam, M. M., M. Moriya and H. Sakamoto (2003). Aerodynamic characteristics of two side-by-side circular cylinders and application of wavelet analysis on the switching phenomenon. *Journal of Fluids and Structures* 18, 325-346.

Alam, M. M., Q. Zheng and K. Hourigan (2017). The wake and thrust by four side-by-side cylinders at a low Re. *Journal of Fluids and Structures* 70, 131–144.

Alam, M. M., Y. Zhou and X. W. Wang (2011). The wake of two side-by-side square cylinders. *Journal of Fluid Mechanics* 669, 432-471.

Bearman, P. W. and A. T. Wadcock (1973). The interaction between a pair of circular cylinders normal to a stream. *Journal of Fluid Mechanics* 61, 499-511.

Bradbury, L. J. S. (1976). Measurements with a pulsed-wire and a hot-wire anemometer in the highly turbulent wake of a normal flat plate. *Journal of Fluid Mechanics* 77, 473-497.

Burattini, P. and A. Agrawal (2013). Wake interaction between two side-by-side square cylinders in channel flow. *Computers & Fluids* 77, 134-142.

Butler, K., S. Cao, A. Kareem, Y. Tamura and S. Ozono (2010). Surface pressure and wind load characteristics on prisms immersed in a simulated transient gust front flow field. *Journal of wind Engineering and Industrial Aerodynamics* 98, 299-316.

Carini, M., F. Giannetti and F. Auteri (2014). On the origin of the flip-flop instability of two side-by-side cylinder wakes. *Journal of Fluid Mechanics* 742, 552-576.

Chatterjee, D. and G. Biswas (2015). Dynamic behavior of flow around rows of square cylinders kept in staggered arrangement. *Journal of Wind Engineering and Industrial Aerodynamics* 136, 1-11.

Chen, L., J. Y. Tu and G. H. Yeoh (2003). Numerical simulation of turbulent wake flows behind two side-by-side cylinders. *Journal of Fluids and Structures* 18, 387-403.

Flachsbart, O. (1935). Der Widerstand quer angeströmter Rechteckplatten bei Reynoldsschen Zahlen 1000 bis 6000, ZAMM - *Journal of Applied Mathematics and Mechanics* 15(1-2), 32-37.

Hacisevki, H. and A. Teimourian (2015). Comparison of flow structures in the wake region of two similar normal flat plates in tandem and a square cylinder. *Experimental Thermal and Fluid Science* 69, 169-177.

Han, Z., D. Zhou, J. Tu, C. Fang and T. He (2014). Flow over two side-by-side square cylinders by CBS finite element scheme of Spalart–Allmaras model. *Ocean Engineering* 87, 40-49.

Hayashi, M., A. Sakurai and Y. Ohya (1986). Wake interference of a row of normal flat plates arranged side by side in a uniform flow. *Journal of Fluid Mechanics* 164, 1-25.

Higuchi, H., J. Lewalle and P. Crane (1994). On the structure of two-dimensional wake behind a pair of flat plates. *Physics of Fluids* 6, 297-305.

Hirano, K., H. Ohsako and A. Kawashima (1983). The interference between two flat plates normal to a stream in staggered arrangement (Part 1). *Transactions of the Japan Society of Mechanical Engineers,* Series B, 49(447), 311-318 (in Japanese).

Kamemoto, K. (1976). Formation and Interaction of Two Parallel Vortex Streets. *Bulletin of the Japan Society of the Mechanical Engineers* 19(129), 283-290.

Kim, H. J. and P. A. Durbin (1988). Investigation of the flow field between a pair of circular cylinders in the flopping regime. *Journal of Fluid Mechanics* 196, 431-448.

Kundu, P. K., I. M. Cohen and D. R. Dowling (2012). *Fluid Mechanics*, 5ed., Academic Press, Boston, USA.

Liu, C-H. and J. M. Chen (2002). Observations of hysteresis in flow around two square cylinders in a tandem arrangement. *Journal of wind Engineering and Industrial Aerodynamics* 90, 1019-1050.

Miau, J. J., G. Y. Wang and J. H. Chou (1992). Intermittent switching of gap flow downstream of two flat plates arranged side by side. *Journal of Fluids and Structures* 6, 563-582.

Mizota, T. (1978). A technique for measuring unsteady flow velocities in the separated region. *Proceedings of the Japan Society of Civil Engineers* 278, 53-60.

Nakaguchi, H. (1972). On Aerodynamic Characteristics and Wake Flows of Bluff Bodies. *Journal of the Japan Society for Aeronautical and Space Science*s 20(226), 22-30 (in Japanese).

Okajima, A. and K. Sugitani (1984). Strouhal number and base pressure coefficient of cylinders with rectangular cross section (Reynolds number effect). *Transactions of the Japan Society of Mechanical Engineers,* Series B, 50-457, 2004-2012 (in Japanese).

Ozono, S., A. Nishi and H. Miyagi (2006). Turbulence generated by a wind tunnel of multi-fan type in uniformly active and quasi-grid modes. *Journal of wind Engineering and Industrial Aerodynamics* 94, 225-240.

Pan, T., L. Zhao, S. Y. Cao, Y. J. Ge and S. Ozono (2011). Analysis of aerodynamic load effect on thin plat section in multiple fan active control wind tunnel. *Procedia Engineering* 14, 2481-2488.

Roshko, A. (1955). On the wake and drag of bluff bodies. *Journal of the Aerospace Sciences* 22, 124-132.

Spivack, H. M. (1946). Vortex frequency and flow pattern in the wake of two parallel cylinders at varied spacings normal to an air stream. *Journal of the Aerospace Sciences* 13, 289-297.

Sumner, D. (2010). Two circular cylinders in cross-

flow. *A review, Journal of Fluids and Structures* 26, 849-899.

Teimourian, A., H. Hacisevki and B. Bahrami (2017). Experimental study on flow past two inclined flat plates in tandem arrangement. *Journal of Wind Engineering and Industrial Aerodynamics* 169, 1-11.

Tong, F., L. Cheng, M. Zhao and H. An (2015). Oscillatory flow regimes around four cylinders in a square arrangement under small and conditions. *Journal of Fluid Mechanics* 769, 298–336.

Wang, Z. J. and Y. Zhou (2005). Vortex interactions in a two side-by-side cylinder near-wake. *Heat and Fluid Flow* 26, 362-377.

Williamson, C. H. K. (1985). Evolution of a single wake behind a pair of bluff bodies. *Journal Fluid Mechanics* 159, 1-18.

Yen, S. C. and J. H. Liu (2011). Wake flow behind two side-by-side square cylinders. *International Journal of Heat and Fluid Flow* 32, 41-51.

Zdravkovich, M. M. (1987). The effects of interference between circular cylinders in cross flow. *Journal Fluids and Structures* 1, 239-261.

Zhao, M. and L. Cheng (2014). Two-dimensional numerical study of vortex shedding regimes of oscillatory flow past two circular cylinders in side-by-side and tandem arrangements at low Reynolds numbers. *Journal of Fluid Mechanics* 751, 1–37.

Zhou, Y. and M. M. Alam (2016). Wake of two interacting circular cylinders. *A review International Journal of Heat and Fluid Flow* 62, 510–537.